Electrochemical Reduction of NO by Myoglobin in Surfactant Film: Characterization and Reactivity of the Nitroxyl (NO^-) Adduct

Mekki Bayachou,† Rong Lin, William Cho, and Patrick J. Farmer*

Contribution from the Department of Chemistry, University of California, Irvine, California 92697-2025

Received March 2, 1998. Revised Manuscript Received June 25, 1998

Abstract: We have examined the electrochemical reduction of NO by myoglobin (Mb) contained within a dimethyldidodecylammonium bromide (ddab) film on pyrolytic graphite electrodes. Immersion of the (Fe^{III})-Mb-doped electrode into aqueous solutions of NO results in a bulk chemical reductive nitrosylation forming NO−Mb−Fe^{II}, as indicated by the dissappearance of the $Fe^{III/II}$−Mb couple in voltammograms. At more negative potentials, a catalytic reduction wave appears at ca. −0.7 V/SCE, which remains catalytic in solutions from pH 5.5 to pH 10 and is NO-concentration dependent. Bulk electrolysis at −0.8 V/SCE of ^{15}NO solutions by Mb/ddab yields $^{15}N_2O$ as gaseous product. Cyclic voltammograms of films made of preformed nitrosyl myoglobin, $MbFe^{II}$−NO, demonstrate a single, reversible reduction to the nitroxyl state, $MbFe^{II}-NO^-$, at $E^\circ = -0.87$ V/SCE. The reversibility of the nitrosyl reduction is pH dependent; digital simulation yields a rate of 22.5 s^{-1} for the irreversible loss of a nitroxyl group at pH 7 and 0.7 s^{-1} at pH 10. The catalytic formation of N_2O during reduction of $MbFe^{II}$−NO in the presence of exogenous NO implies that an N−N coupling reaction occurs at the active site between the Fe-bound nitroxyl and a free NO. A mechanism is proposed for the catalysis involving decomposition of an ($N_2O_2^-$)−Fe^{II}−Mb intermediate.

Introduction

Nitric oxide (NO) binding to heme proteins has been linked to a number of important physiological processes such as vasodilation,[1a] neurotransmission,[1b] and cytotoxicity.[1c] Such interactions are also crucial in microbial denitrification, the biological transformation of nitrite into the gases N_2O and N_2.[2] Free NO has been identified as an obligate intermediate in many denitrifying bacteria; Fe heme as well as Cu nitric oxide reductases (NoR) have been identified, but the mechanisms by which two NO molecules are coupled is still much debated.[2−4] In this regard, several metalloporphyrins have been reported to act as electrocatalysts for the reduction of NO.[5,6]

We are interested in following reductive catalysis by heme proteins using surfactant film methodology, as developed by Rusling.[7] In this procedure, the single-heme protein myoglobin (Mb) is contained within a thin film (ca. 1 μm) of a water-insoluble surfactant, dimethyldidodecylammonium bromide (ddab), on a pyrolitic graphite electrode. The electrochemical response of Mb in such a film is greatly enhanced compared with that of Mb in solution and exhibits a scan-rate dependence indicative of Mb diffusion through the surfactant film.[7a] A number of spectroscopic techniques indicate that Mb retains its native structure within the film environment.[8]

Taking advantage of the fast electrochemical response of such Mb/ddab electrodes, we recently reported the electrocatalytic reduction of nitrite in buffered media.[9] The products of nitrite reduction by Mb/ddab (NH_4^+, NH_3OH^+, as well as the gaseous products N_2O, NO, and N_2) are similar to those made enzymatically by nitrite and nitric oxide reductases.[9a] Because of the possible intermediacy of NO in this reactivity, we have examined NO reduction by Mb/ddab modified electrodes under both catalytic and single-turnover conditions and analyzed its behavior as a model for heme-based NoR reactivity.

Experimental Section

Materials. Lyophilized myoglobin from horse skeletal muscle was obtained from Sigma and purified as in ref 8d. ddab was purchased from Acros. Pyrolytic graphite (PG) was purchased from Union Carbide, cut into basal-plane oriented disks, and fabricated into

† On postdoctoral stay from Laboratoire de l'eau et de l'environnement, Department de Chimie,Université Chouaïb Doukkali, B.P. 20, El Jadida, Morocco.

(1) (a) Clancy, R. M.; Abramson, S. B. *Proc. Soc. Exp. Biol. Med.* **1995**, *210*, 93. (b) Tsai, A.-L. *FEBS Lett.* **1994**, *341*, 141. (c) Kurata, S.; Matsumoto, M. Yamashita, U. *J. Biochem. (Tokyo)* **1996**, *120*, 49.

(2) Payne, W. J. In *Denitrification*; John Wiley & Sons: New York, 1981.

(3) (a) Averill, B. A. *Chem. Rev.* **1996**, *96*, 2951. (b) Ye, R. W.; Averill, B. A.; Tiedje, J. M. *Appl. Environ. Microbiol.* **1994**, *60*, 1053. (c) Averill, B. A.; Tiedje, J. M. *FEBS Lett.* **1982**, *138*, 8.

(4) (a) Dermastia, M.; Turk, T.; Hollocher, T. C. *J. Biol. Chem.* **1991**, *266*, 10899. (b) Zumft, W. G. *Arch. Microbiol.* **1993**, *160*, 253. (c) Kastrau, D. H. W.; Heis, B.; Kroneck, P. M. H.; Zumft, W. G. *Eur. J. Biochem.* **1994**, *222*, 293.

(5) (a) Murphy, W. R., Jr.; Takeuchi, K.; Barley, M. H.; Meyer, T. J. *J. Am. Chem. Soc.* **1982**, *104*, 5817. (b) Barley, M. H.; Takeuchi, K.; Meyer, T. J. *J. Am. Chem. Soc.* **1986**, *108*, 5876. (c) Barley, M. H.; Rhodes, M. R.; Meyer, T. J. *Inorg. Chem.* **1987**, *26*, 1746. (d) Younathan, J. N.; Wood, K. S.; Meyer, T. J. *Inorg. Chem.* **1992**, *31*, 3280.

(6) (a) Liu, Y.; Ryan, M. D. *J. Electroanal. Chem.* **1994**, *368*, 209. (b) Cheng, S. H.; Su, Y. O. *Inorg. Chem.* **1994**, *33*, 5847. (c) Yu, C.-H.; Su, Y. O. *J. Electroanal. Chem.* **1994**, *368*, 323.

(7) (a) Rusling, J. F.; Nassar, A. E. F. *J. Am. Chem. Soc.* **1993**, *115*, 11891. (b) Nassar, A. E. F.; Bobbitt, J. M.; Stuart, J. D.; Rusling, J. F. *J. Am. Chem. Soc.* **1995**, *117*, 10986.

(8) (a) Rusling, J. F.; Nassar, A. E. F.; Kumosinski, T. F. In *Molecular Modeling: from virtual tools to real problems*; Kumosinski, T. F., Liebman, M. N., Eds.; ACS Symposium Series 576; American Chemical Society: Washington, DC, 1994; p 250. (b) Nassar, A. E. F.; Zhang, Z.; Chynwat, V.; Frank, H. A.; Rusling, J. F.; Suga, K. *J. Phys. Chem.* **1995**, *99*, 11013. (c) Nassar, A. E. F.; Narikiyo, Y.; Sagara, T.; Nakashima, N.; Rusling, J. F. *J. Chem. Soc., Faraday Trans.* **1995**, *91*, 1775. (d) Nassar, A.-E. F.; Willis, W. S.; Rusling, J. F. *Anal. Chem.* **1995**, *67*, 2386.

(9) (a) Lin, R.; Bayachou, M.; Greaves, J.; Farmer, P. J. *J. Am. Chem. Soc.* **1997**, *119*, 12689. (b) Farmer, P. J.; Lin, R.; Bayachou, M. *Comments Inorg. Chem.* **1998**, *20*, 101.

S0002-7863(98)00697-0 CCC: $15.00
Published on Web 09/05/1998

homemade electrodes as per ref 7a. All other chemicals were reagent grade. Nitric oxide gas was generated from sulfuric acid and sodium nitrite[10] or from Air Gas and then passed through an azide solution trap to remove NOx impurities. ^{15}N-Labeled sodium nitrite was obtained from Cambridge Isotope Laboratories. A Barnstead Nanopure system was used to purify water to a specific resistance of greater than 18 MΩ cm.

Mb/ddab Film Preparation. A 0.046-g sample of ddab in 15 mL of water (0.01 M) was suspended and ultrasonicated for at least 6 h until the solution became clear. A 10-μL portion of 0.01 M ddab solution and 10 μL of a 0.5 mM metMb (Fe^{III}) solution were cast onto the surface of a basal-plane oriented PG electrode. The Mb/ddab films were dried in a closed vessel overnight and then exposed to air for a minimum of 12 h.

Nitrosyl myoglobin films (NO−Mb/ddab) were prepared similarly with the following modifications: NO−Mb was generated under anaerobic conditions in a glovebox by the addition of $NaNO_2$ and NaS_2O_4 to a freshly prepared solution of metmyoglobin;[11] the resulting NO−Mb solution was purified on a Sephadex G25 column. An ultrasonicated solution of ddab (10 mM) was thoroughly degassed prior to transfer to the glovebox. NO−Mb/ddab films were made by casting ~20 μL of a mixture of equal volumes of ddab solution and NO−Mb (ca. 0.6 mM) onto freshly polished PG electrodes. The film is maintained under a closed vessel overnight and then allowed to dry in the glovebox.

Voltammetry. A BAS 100W electrochemical analyzer was used with a standard three-electrode cell, consisting of a Pt wire counter electrode, a saturated calomel reference electrode (SCE) connected via Luggin capillary to the analyte solution, and a basal-plane pyrolytic graphite (PG) disk working electrode. PG cylinders (Union Carbide) were sealed with epoxy into glass tubes and connected to a wire with Ag paste. All electrochemical experiments were performed at room temperature (22 ± 2 °C). The electrodes were immersed into solutions containing a 0.1 or 0.5 M NaBr electrolyte. For the Mb/ddab electrodes, the analyte solution was purged with purified nitrogen for at least 20 min to remove oxygen prior to the beginning of each series of experiments, and a nitrogen atmosphere was maintained over the solution during all experiments. Voltammograms of the NO−Mb/ddab film electrodes were run under similar conditions without purging in an anaerobic glovebox. Digital simulations of voltammograms used the BAS Digisim program.

Ferric Mb Reduction by NO. A 10-mL three-necked round-bottomed flask was filled with 6 mL of buffer solution (pH 5.5 citrate buffer, phosphate buffer from 6 to 9, and pH 10 borate buffer), with 0.1 M KCl as an electrolyte. The solutions were degassed for 10 min, and the gas outlet was closed with positive N_2 pressure. For dilute NO solutions, aliquots of a saturated NO solution were directly added to the electrochemical analyte solution via a gastight syringe. The concentrations reported assume that the diffusion of dissolved NO into the small volume of headgas (<5 mL) is slow and does not affect the calculated values. To minimize the effect of electrode history, a freshly made electrode was used for each experiment. The bulk reduction of Fe^{III}Mb was followed by rapid scan voltammetry (typically 500 mV/s) every 30 s.

Bulk Electrolysis. Bulk electrolysis reactions and product analysis were carried out as in ref 7a, with NO gas introduced into the electrolysis solution by bubbling. Pyrolytic graphite plates (1.0 × 1.0 × 0.2 cm) coated with Mb/ddab were used as working electrodes. Controlled potential was applied by using a BAS 100W and a Power Module potentiostat, a SCE reference, and a Pt grid counter electrode separated by a fine frit from the main compartment. ^{15}NO was generated by treating $Na^{15}NO_2$ with $Fe(SO_4)/H_2SO_4$ acid using the procedure in ref 10. A He carrier gas was used to transfer the continuously generated ^{15}NO into the electrolysis cell through a fused silica line. The headgas over the electrolysis solution was sampled in a loop and transferred directly into a Micromass Autospec mass spectrometer via a GC interface through a Plot GC Column (fused silica 50 m × 0.32 mm, Al_2O_3, KCl coating). Data were acquired in EI mode at 1000 resolution.

(10) Cotton, F. A.; Wilkinson, G. In *Advanced Inorganic Chemistry*, 5th ed.; John Wiley & Sons: New York, 1988; p 321.

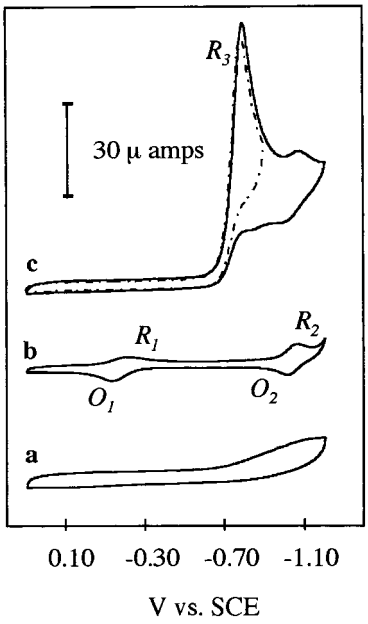

Figure 1. Cyclic voltammograms in deareated pH 7.4 buffer (50 mM NaBr, 500 mV/s): (a) ddab film electrode in saturated NO solution; (b) Mb/ddab film electrode; (c) solid line, Mb/ddab film electrode in saturated NO solution; dotted line, with scan direction switched after R_3.

Absorbance Spectra. UV−vis spectra were obtained using a Hewlett-Packard 8453 spectrometer. Films were deposited onto quartz slides and dried under inert atmosphere, following the same procedure as on electrodes. In an anaerobic quartz cuvette containing a pH 7 buffer, an NO−Mb/ddab and a control ddab film cast on quartz slides were placed at a right angle to each other. The cuvette was maintained under N_2, and the UV−vis spectrum through each immersed plate was recorded with the NO−Mb spectra derived from their difference.

Results

As previously reported, cyclic voltammograms of Mb/ddab electrodes show two reduction couples in pH 7 buffered solutions, Figure 1b.[7−9] The first, R_1/O_1 with $E°_1 = -0.22$ V/SCE, is assigned to the Fe^{III}/Fe^{II} couple of Mb.[7a] The second couple, R_2/O_2, tentatively assigned to the Fe^{II}/Fe^{I} couple of Mb,[7b] occurs at $E°_2 = -1.09$ V/SCE. In cyclic voltammograms taken upon immersion of an Mb/ddab electrode into aqueous NO(g) saturated solutions, the voltammetric currents at the R_1/O_1 wave disappear, and a new catalytic wave appears, R_3, at ca. −0.75 V/SCE, Figure 1c. This wave remains catalytic (i.e., multiple electrons per Fe) from pH 5.5 to pH 10.[12] As an NO-saturated analyte solution is degassed with N_2, the R_3 peak current decreases and the R_1/O_1 couple reappears during sequential cyclic voltammograms.[13]

Voltammograms under NO change with increasing scan rate, Figure 2. At scan rates over 200 mV/s, a small oxidation wave corresponding to O_1 is present after scanning through R_3, Figure 2b. At faster scan rates, e.g., 10 V/s, an anodic wave, O_3, appears following R_3, Figure 2c. Qualitatively, the current at O_3 decreases with increasing H^+ and NO concentration. At low NO concentrations, waves are evident for the starting Mb (R_1/O_1 and R_2/O_2) in addition to the catalytic wave at R_3.

The initial disappearance of the E_1 couple upon exposure to NO was followed using dilute solutions, Figure 3. In 30-μM

(11) Arnold, E. V.; Bohle, D. S. In *Methods in Enzymology*; Packer, L., Ed.; Academic Press: San Diego, 1996; Vol. 268, Part B; pp 41−55.

(12) Nassar, A.-E.; Zhang, Z.; Hu, N.; Rusling, J. F.; Kumosinski, T. F. *J. Phys. Chem.* **1997**, *101*, 2224.

(13) These voltammograms can be found in the Supporting Information.

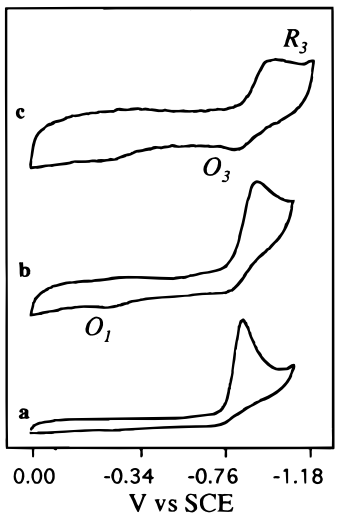

Figure 2. Cyclic voltammograms of reduction of a Mb/ddab film electrode in saturated NO solution, pH 5.5 illustrating the scan rate dependence: (a) 200 mV/s; (b) 1 V/s c) 10 V/s.

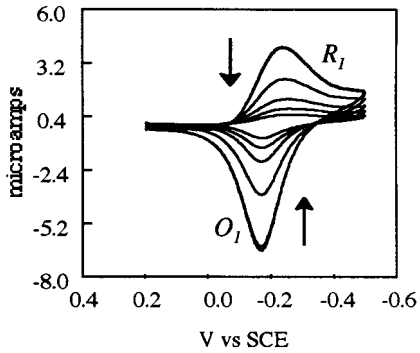

Figure 3. Consecutive voltammograms showing the loss of $E_1°$ couple after addition of NO to analyte solution, as described in the Experimental Section. Conditions: scan rate 500 mV/s, 0.03 mM NO, pH 7.

NO solutions, the current at R_1/O_1 disappeared over several minutes at all pHs tested. The rates of the E_1 disappearance were pH dependent and somewhat dependent also on electrode history.

Controlled-potential electrolysis using large PG-plate Mb/ddab electrodes was used to determine the products of the catalysis. During electrolysis, the headgas above the analyte solution was continuously sampled into a mass spectrometer through a GC interface. In saturated ^{15}NO solutions at pH 5.5, electrolysis at potentials corresponding to R_3 yields a strong signal at $m/z = 46$, corresponding to $^{15}N_2O$; no signal was evident at potentials more positive to R_3, i.e., at potentials > -500 mV SCE. Aliquots of the analyte solution taken during electrolysis were examined after thorough degassing for nitrite and ammonia by standard colorimetric tests.[14] A small, variable amount of nitrite was found to be formed during electrolysis; no ammonia was detected.

NO−Mb/ddab films were cast under anaerobic conditions from preformed and purified nitrosyl myoglobin. Such films cast on quartz yield Soret absorbance identical to that of NO−Mb in aqueous solution, Figure 4.[15] Cyclic voltammetry of these films at pH 10, Figure 5a, obtains a reversible reduction couple, R_3/O_3, at $E°_3 = -0.87$ V/SCE. Upon scanning through the R_2/O_2 couple at < -1 V, the current at O_3 is substantially decreased and the R_1/O_1 currents are regained, Figure 6. Once lost, the R_3/O_3 current is never regained under these conditions. At lower pH, scan rates must be increased to maintain the reversibility

(14) Colorimetric determinations of NH_3 and HNO_2 tests were performed as in ref 7a.

(15) We have no evidence of NO−Mb denaturation induced by ddab under our conditions: Das, T. K.; Mazumdar, S.; Mitra, S. *J. Chem. Soc., Chem. Commun.* **1993**, 1447.

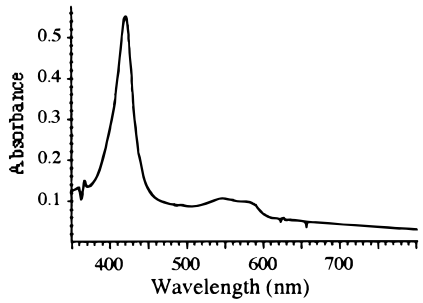

Figure 4. Absorbance spectra of preformed NO−Mb/ddab film on quartz, as described in the text.

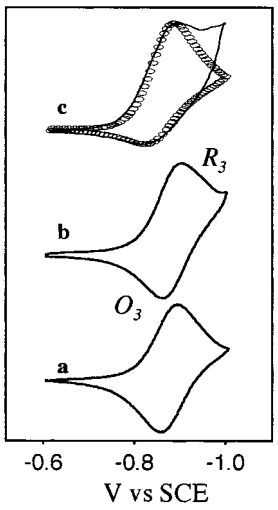

Figure 5. Voltammograms showing reversibility of NO−Mb reduction in different pH solutions: (a) pH 10, at a scan rate of 20 mV/s; (b) pH 8.6, 1 V/s; (c) pH 7, 3 V/s (simulation is shown in circles).

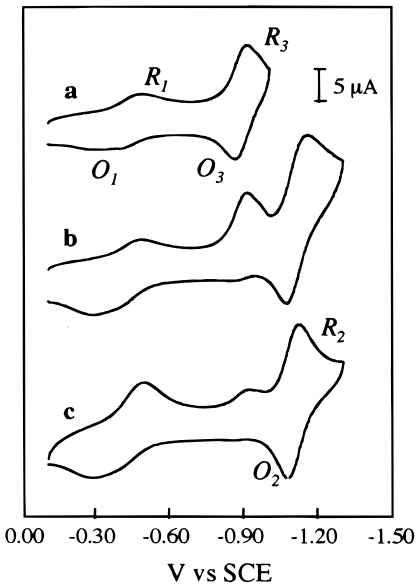

Figure 6. Consecutive voltammograms of a NO−Mb/ddab film electrode illustrating the conversion to Mb/ddab; all voltammograms at 200 mV/s in pH 10 buffer, starting at −100 mV and scanning negatively: (a) first scan, reversed before E_2 at −1 V; (b) second scan, reversed after E_2 at −1.2 V; (c) third scan, reversed after E_2.

of R_3/O_3, Figure 5b. At pH 7.0, the return wave O_3 is substantially diminished even at 3 V/s, Figure 5c. Again, the loss of current at O_3 yields the concurrent increase in the R_1/O_1 current.

Discussion

Formation of NO−Mb. Upon immersion of a Mb/ddab electrode into a solution saturated in NO, the E_1 wave corresponding to the $Fe^{III/II}$ reduction disappears owing to a bulk chemical reduction of Fe^{III}−Mb by NO, ultimately forming NO−Fe^{II}−Mb. Once formed, the Fe^{II}−NO state is stable to oxidation within our solvent window, to +0.4 V SCE. Similar reductive nitrosylations have been reported for a number of heme proteins and model complexes in hydroxylic solvents.[16,17] In a recent paper, Hoshino et al. have investigated the pH dependence of this process for heme proteins in aqueous solutions.[17] In the proposed mechanism, the reduction is initiated by a nucleophilic attack of hydroxide or water on the NO adduct of Fe^{III}−heme; loss of nitrite and subsequent NO binding forms the stable ferrous nitrosyl, eqs 1−3. The pH dependence is quite different for the proteins examined; e.g., Mb and cytochrome *c* are stable to reduction below pH 7, reversibly forming Fe^{3+}−NO adducts, while ferric Hb solutions are irreversibly reduced even below pH 6.

$$Fe^{III}\text{−heme} + NO \rightleftharpoons NO\text{−}Fe^{III}\text{−heme} \quad (1)$$

$$NO\text{−}Fe^{III}\text{−heme} + OH^- \rightarrow Fe^{II}\text{−heme} + HNO_2 \quad (2)$$

$$Fe^{II}\text{−heme} + NO \rightarrow NO\text{−}Fe^{II}\text{−heme} \quad (3)$$

By comparison, the overall rate of reductive nitrosylation of Mb/ddab is several orders of magnitude faster than Mb in solution. We followed the reduction under dilute NO solutions (0.03 mM), using the current at O_1 as an indicator of Fe^{III} myoglobin concentration, Figure 3.[18] The ferric Mb/ddab is reduced within several minutes from pH 6 to 10. The plot of the natural logarithm of current vs time gives a pseudo-first-order rate constant of 0.032 s^{-1} for the overall reductive nitrosylation at pH 7.

The more hydrophobic nature of the surfactant film environment most certainly alters the progress of the reaction by affecting the activities and concentrations of the reactants. For example, the actual concentration of NO in the ddab film is likely different than in solution, as NO is ca. 70 times more soluble in hydrophobic solvents than in aqueous solutions.[19] The reactivity of Mb in ddab may likewise be affected by changes in the protein's conformational mobility and solvent access to the heme site, but still it mirrors that of the native active site. A number of spectroscopic measurements, such as IR and EPR, show that the secondary structure and heme ligation of Mb in the such films is comparable to solution-based Mb.[8,12] Chemical modification of the distal pocket produces a dramatic change in the electrochemical response, again confirming the electroactive species is the folded, native protein.[9b] Likewise, the heme environment as measured by Soret absorbances of ligand adducts of native and chemically modified Mb remains similar to that of Mb in aqueous solution.[7,9b]

Table 1. Reduction Potentials for NO−Fe Porphyrin Complexes

model complex	$E°$ vs SCE	solvent
NOFe(tetraphenylporphyrin)[20]	−0.93	CH_2Cl_2
NOFe(tetrakis(4-sulfonatophenyl)porphyrin)[21]	−0.63 (irrev)[a]	water
NOFe(octaethylporphyrin)[20]	−1.08	CH_2Cl_2
NOFe(2,4-octaethylporphyrindione)[22]	−0.69	THF

[a] Peak potential of an irreversible reduction wave.

Catalytic Reduction of NO. In voltammograms of Mb/ddab scanned to more negative potentials under NO solutions, a large reductive current is seen, Figure 1c, corresponding to the catalytic reduction of NO. The catalysis is efficient under saturated NO conditions: the current wave increases with decreasing scan rate, but a limiting current value indicative of steady-state catalysis was never reached. The products of catalysis were determined after bulk electrolysis of NO saturated solutions. For gaseous products, labeled ^{15}NO was used to avoid interference from atmospheric gases in the GC/MS of the headgas above the electrolysis. A strong signal corresponding to $^{15}N_2O$ was seen upon electrolysis at −800 mV; no other gaseous ^{15}N-labeled products were seen. Analysis of the aqueous electrolysis solution showed that nitrite was also formed during catalysis (vide infra). No further reduction products, such as ammonia or hydroxylamine, were found.

The ability to obtain good current response during fast voltammetric scans of Mb/ddab films allowed more detailed analysis of the catalysis. At scan rates over 200 mV/s, a small oxidation wave corresponding to O_1 is present after scanning through R_3, indicating Fe^{II}−Mb is generated during catalysis, Figure 2b. At faster scan rates under catalytic conditions in Figure 2c, the appearance of O_3 is the kinetic fingerprint of a chemically reversible reduction; i.e., O_3 is due to the reoxidation of the reduced form of $MbFe^{II}$−NO before the catalytic following reaction.

Reversibility of Nitrosyl Reduction. Owing to the inherent difficulty in limiting and measuring the NO concentrations in ddab films, we attempted single-turnover reduction experiments using preformed and purified $MbFe^{II}$−NO cast in ddab films. As Figure 5 clearly indicates, $MbFe^{II}$−NO in such films undergoes a single, reversible reduction, eq 4. The standard

$$NO\text{−}Fe^{II}\text{−Mb} + e^- \rightleftharpoons (NO^-)\text{−}Fe^{II}\text{−Mb} \quad (4)$$

reduction potential, $E° = -0.87$ V/SCE (−0.63 V/NHE), falls within the range of previously reported values of NO adducts of Fe−porphyrin compounds, Table 1.[20−22] The heterogeneous electron-transfer rate for the E_3 wave, at 9.3×10^{-2} cm/s, is larger than the metal-centered reduction E_1, at 8.9×10^{-3} cm/s, suggesting a ligand-centered reduction.[23] A reasonable formulation of the reversibly formed species is nitroxyl myoglobin, $MbFe^{II}$−NO^-, in which the reducing electron resides in a hybrid Fe−NO orbital.[22,24] To our knowledge, this is the

(16) (a) Wayland, B. B.; Olson, L. W. *J. Am. Chem. Soc.* **1974**, *96*, 6037. (b) Scheidt, W. R.; Frisse, M. E. *J. Am. Chem. Soc.* **1975**, *97*, 17. (c) Yoshimura, T.; Suzuki, S.; Nakahara, A.; Iwasaki, H.; Masuko, M.; Matsubara, T. *Biochemistry* **1986**, *25*, 2436.

(17) Hoshino, M.; Maeda, M.; Konishi, R.; Seki, H.; Ford, P. C. *J. Am. Chem. Soc.* **1996**, *118*, 5702.

(18) A fast scan rate and minimum number of scans were used to prevent perturbation of the bulk reaction rate by electrochemical reduction and binding of NO in the electroactive layer. Further data from the reductive nitrosylation of Mb/ddab at pH 6−8 are given in the Supporting Information.

(19) Lancaster, J. R., Jr. In *Methods in Enzymology*; Packer, L., Ed.; Academic Press: San Diego, 1996; Vol. 268, Part A; pp 31−50.

(20) (a) Lancon, D.; Kadish, K. M. *J. Am. Chem. Soc*. **1982**, *104*, 2042. (b) Lancon, D.; Kadish, K. M. *J. Am. Chem. Soc.* **1983**, *105*, 5610.

(21) Barley, M. H.; Takeuchi, K.; Meyer, T. J. *J. Am. Chem. Soc*. **1986**, *108*, 5876.

(22) Liu, Y. M.; Desilva, C.; Ryan, M. D. *Inorg. Chim. Acta* **1997**, *258*, 247.

(23) The k_{et} for eq 6 was estimated from scans at 1, 5, and 20 V/s. Similar variability in heterogeneous electron-transfer rates have been used to differentiate between metal- and porphyrin-based reductions: Mu, X. H.; Schultz, F. A. *Inorg. Chem.* **1990**, *29*, 2877.

first direct electrochemical characterization of a ferrous−nitroxyl adduct of a hemeprotein.

Although Fe−porphyrin nitroxyls may undergo an additional reversible reduction in organic solvents,[25] further reduction of $MbFe^{II}-NO^-$ leads to irreversible loss of the NO−Mb/ddab and reformation of the unligated Mb/ddab, Figure 6. The R_1/O_1 couple is shifted and broadened owing to the binding of OH^- to Mb at the open coordination site.[12] The potential and reversibility of the E_2 wave following the nitroxyl formation suggests that the nitroxyl ligand dissociates concurrent with or rapidly following the electron transfer, generating Fe^I, eq 5.

$$(NO^-)-Fe^{II}-Mb + e^- \rightarrow Fe^{I}-Mb + NO^- \quad (5)$$

The lifetime of the nitroxyl state is pH dependent; at lower pH the E_3 couple is reversible only at faster scan rates, Figure 5b. Digital simulation of the NO−Mb/ddab voltammogram at pH 7, c (circles), yields a rate of 22.5 s^{-1} for the irreversible loss of the Fe-coordinated NO, regenerating the uncomplexed Mb/ddab current signals (the current rise past the E_3 peak in Figure 5b,c is due to the E_2 peak of unligated Mb). At pH 10, the rate of the following reaction is less than 0.7 s^{-1}, Figure 5a. These results are comparable with the 2 s half-life recently reported for a nitroxyl adduct generated by flash photolytic reduction of NO−Fe(tpps) in aqueous solution.[26]

N_2O Formation. The pH dependence of the nitroxyl adduct's lifetime suggests it can decompose by loss of HNO ($pK_a = 4.7$),[27] which may then rapidly couple in solution to form N_2O, eq 7. Such a mechanism has been proposed by Hollocher as a nonenzymatic pathway to N_2O formation from the heme bc_1 NoR enzymes.[4]

$$(NO^-)-Fe^{II}-Mb + H^+ \rightarrow Fe^{II}-Mb + HNO \quad (6)$$

$$2HNO \rightarrow N_2O + H_2O \quad (7)$$

In an alternative solution-based coupling, NO^- can react sequentially with two NO molecules, eqs 8−10.[27] By this mechanism, one reduction equivalent leads to concomitant formation of NO_2^- and N_2O, eq 10. We have analyzed for aqueous products after numerous experiments and found low-level production of nitrite during Mb/ddab-catalyzed NO electrolysis, on average equivalent to 7% of the current passed.[28] This may be attributable to a background of uncatalyzed reduction of NO by this mechanism or to leakage from NO oxidation within the counter-electrode compartment. Significantly, in control experiments using ddab film electrodes without Mb, greater than 50% of the current equivalent of nitrite was formed. The stoichiometric reductive nitrosylation of $Fe^{III}Mb$, eq 2, would generate less than 0.1% nitrite compared to catalytic currents measured.

$$NO^- + NO \rightleftharpoons N_2O_2^- \qquad k_{forward} = 2 \times 10^9\ M^{-1}\ s^{-1} \quad (8)$$

$$N_2O_2^- + NO \rightleftharpoons N_3O_3^- \qquad k_{forward} = 5 \times 10^6\ M^{-1}\ s^{-1} \quad (9)$$

$$N_3O_3^- \rightarrow N_2O + NO_2^- \qquad k = 87\ s^{-1} \quad (10)$$

Comparison of the reversible reduction of NO−Mb/ddab seen in Figure 5 with its efficient and relatively pH-independent catalytic reaction in the presence of exogenous NO, Figure 1, implies that the coordinated nitroxyl reacts with NO, as in eqs 11 and 12.

$$(NO^-)-Fe^{II}-Mb + NO \rightarrow (N_2O_2^-)-Fe^{II}-Mb \quad (11)$$

$$(N_2O_2^-)-Fe^{II}-Mb + e^- + 2H^+ \rightarrow N_2O + H_2O + Fe^{II}-Mb \quad (12)$$

In this hypothesis, the stable nitroxyl adduct reacts with NO to form an Fe-bound $N_2O_2^-$ intermediate, eq 11, which ultimately leads to N_2O formation.[29] The details of the transformations included in eq 12, such as their sequence and pH dependence, are under further investigation. A simplified reaction scheme for the overall catalysis, eq 13−16, has been used to simulate the voltammogram in Figure 1c, yielding a rate for the coupling reaction, k_{cat}, of $2 \times 10^8\ M^{-1}\ s^{-1}$.[30]

$$NO-Fe^{II} + e^- \rightleftharpoons (NO^-)-Fe^{II} \quad (13)$$

$$(NO^-)-Fe^{II} + NO \xrightarrow{k_{cat}} Fe^{III} + \text{products} \quad (14)$$

$$Fe^{III} + e^- \rightleftharpoons Fe^{II} \quad (15)$$

$$Fe^{II} + NO \rightleftharpoons NO-Fe^{II} \quad (16)$$

The proposed intermediate, $(N_2O_2^-)-Fe^{II}-Mb$, is analogous to the well-known NONOate salts formed from N−N catenation upon exposure of anionic nucleophiles to NO.[31−33] A ferrous NONOate may be expected to be unstable, decomposing by innersphere electron transfer to give $N_2O_2^{2-}$ and Fe^{III}. Once formed, the aqueous hyponitrite, $N_2O_2^{2-}$, would rapidly generate N_2O below pH 10. A comparable transformation occurs for the sulfite-derived NONOate, $SO_3N_2O_2^{2-}$, which decomposes (via loss of $N_2O_2^{2-}$) to form sulfate and nitrous oxide, eq 17.[33a] In contrast, dialkylamine NONOates, such as the diethylamine adduct, decompose to give 2 equiv of NO, eq 18.[33b]

$$(SO_3)N_2O_2^{2-} \rightarrow SO_4^{2-} + N_2O \quad (17)$$

$$(Et_2N)N_2O_2^- \rightarrow Et_2N^- + 2NO \quad (18)$$

In the biochemical literature, a number of mechanisms have been proposed for the production of N_2O during denitrifica-

(24) Waleh, A.; Ho, N.; Chantranupont, L.; Lowe, G. H. *J. Am. Chem. Soc.* **1989**, *111*, 2767.

(25) Choi, I.-K.; Liu, Y.; Feng, D. W.; Paeng, K.-J.; Ryan, M. D. *Inorg. Chem.* **1991**, *30*, 1832.

(26) [tpps = *meso*-tetrakis(*p*-sulfonatophenyl)porphyrinate]: Seki, H.; Hoshino, M.; Kounose, S. *J. Chem. Soc., Faraday Trans.* **1996**, *92*, 2579.

(27) Gratzel, V. M.; Taniguchi, S.; Henglein, A. *Ber. Bunsen-Ges. Phys. Chem.* **1970**, *74*, 1003.

(28) In these experiments, rapid freezing of the electrolysis solution followed by lyophilization were performed to prevent NO_2^- formation by reaction of NO with adventitious O_2: Wink, D. A.; Darbyshire, J. F.; Nims, R. W.; Saavedra, J. E.; Ford, P. C. *Chem. Res. Toxicol.* **1993**, *6*, 23.

(29) Similar intermediates have been proposed to result from electrophilic attack of NO on Co and Pd nitrosyls: (a) MacNeil, J. H.; Berseth, P. A.; Bruner, E. L.; Perkins, T. L.; Wadia, Y.; Westwood, G.; Trogler, W. C. *J. Am. Chem. Soc.* **1997**, *119*, 1668. (b) Gwost, D.; Caulton, K. G. *Inorg. Chem.* **1974**, *13*, 414.

(30) Further details regarding the simulations, including the kinetic parameters used, are given in the Supporting Information.

(31) (a) Drago, R. S. In *Free Radicals in Inorganic Chemistry*; Advances in Chemistry Series 36; American Chemical Society: Washington, DC, 1962; Chapter 15. (b) Longhi, R.; Drago, R. S. *Inorg. Chem.* **1962**, *1*, 768.

(32) Keefer, L. K.; Christodoulou, D.; Dunams, T. M.; Hrabie, J. A.; Maragos, C. M.; Saavedra, J. E.; Wink, D. A. In *Nitrosamines and Related N-Nitroso Compounds*; Loeppky, R. N., Michejda, C. J., Eds.; ACS Symposium Series, 553; American Chemical Society: Washington, DC, 1994; Chapter 11.

(33) (a) Switkes, E. G.; Dasch, G. A.; Ackermann, M. N. *Inorg. Chem.* **1973**, *12*, 1120. (b) Maragos, C. M.; Morley, D.; Wink, D. A.; Dunams, T. M.; Saavedra, J. E.; Hoffman, A.; Bove, A. A.; Isaac, L.; Hrabie, J. A.; Keefer, L. K. *J. Med. Chem.* **1991**, *34*, 3242.

Scheme 1

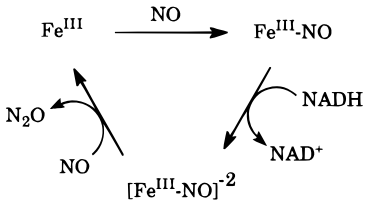

tion: the coupling of two metal-bound nitrosyls,[3b] nucleophilic attack of nitrite on an Fe^{III}−nitrosyl,[3c] and the solution-based coupling of HNO released after reduction of Fe^{II}−nitrosyls.[4a] Recently, a fungal nitric oxide reductase, P450nor, has been reported, in which a spectroscopically identified intermediate, corresponding to the two electron reduction of Fe^{III}−NO, has a lifetime that is attenuated by increased NO concentrations, Scheme 1.[34] Our results suggest a similar reactivity, i.e., the coupling of heme-bound nitroxyl with exogenous NO leading to N_2O formation.

Conclusion

We have utilized electroactive myoglobin in surfactant films to model reductive coupling of NO during denitrification by heme-based enzymes. The surfactant film methodology enables rapid-scan voltammetry and, thus, the direct electrochemical characterization of short-lived intermediates. Significantly, we find that the nitroxyl−myoglobin adduct has a half-life of seconds at high pH, but decomposes by reaction with H^+ or NO. Work is underway to further characterize the reactivity of the nitroxyl adduct, which may be an important intermediate in *N*-oxide reductases at a branching point between pathways leading to the gaseous N−N coupled products and the more reduced aqueous products such as NH_3.[9b]

Acknowledgment. We thank Dr. John Greaves for valued discussions and mass spectroscopic analysis and Dr. Don Blake for use of a PLOT GC column. This research was supported by the National Science Foundation (CHE-9702332), the Petroleum Research Fund (PRF-31804-G3) and startup funding from the University of California, Irvine. M.B. thanks the IDB for post-doctoral support.

Supporting Information Available: Voltammograms illustrating the NO concentration dependence of the catalytic reductions, pH dependence of the bulk reduction of Mb/ddab by NO, and an explanation of parameters and equations used in simulating voltammograms (3 pages, print/PDF). See any current masthead page for ordering information and Web access instructions.

JA980697C

(34) (a) Shiro, Y.; Fujii, M.; Iizuka, T.; Adachi, S. I.; Tsukamoto, K.; Nakahara, K.; Shoun, H. *J. Biol. Chem.* **1995**, *270*, 1617. (b) Shiro, Y.; Fujii, M.; Isogai, Y.; Adachi, S.-i.; Iizuka, T.; Obayashi, E.; Makino, R.; Nakahara, K. Shoun, H.; *Biochemistry* **1995**, *34*, 9052. (c) Nakahara, K.; Tamimoto, T.; Hatauro, K.; Usuda, K.; Shoun, H. *J. Biol. Chem.* **1993**, *268*, 8350.